

Received 16 March 2023, accepted 31 March 2023, date of publication 7 April 2023, date of current version 17 April 2023.

Digital Object Identifier 10.1109/ACCESS.2023.3265468

RESEARCH ARTICLE

Rain-Based Attenuation and Dispersion Characteristics of Terahertz Wave in Tropical Climate: Experimentally Verified Reliability Study

DEBRAJ CHAKRABORTY¹, SAJITH D. NAIR, AND MOUMITA MUKHERJEE¹, (Member, IEEE)

Department of Physics, School of Basic and Applied Sciences, Adamas University, Kolkata, West Bengal 700126, India

Corresponding author: Moumita Mukherjee (drmmukherjee07@gmail.com)

This work was supported by the Defence Research and Development Organization (DRDO), Ministry of Defence, Government of India, under Grant ERIP/ER/202101001/M/01/1780.

ABSTRACT In the frontier of next generation communication system, the terahertz spectrum can be treated un-parallel as far as the implementation of wireless link with high data-rate is concerned. Atmospheric condition can affect the electromagnetic/radio signal transmission severely. Since, the presence of seasonal hydrometeors in atmosphere may lead to drastic degradation in the free-space propagation of terahertz signal, therefore thorough and comprehensive investigation is essentially required to optimize the future channel-model for terahertz carrier frequency. The atmospheric attenuation causes power loss and in turn receiver signal amplitude gets attenuated. Rain attenuation has pronounced impact on terahertz signal propagation and attenuation of transmitted wave. In tropical weather scenario, the drop-dimension of seasonal rainfall exceeds the maximum dimension of temperate rain. Through an indigenously developed and experimentally verified Non-Linear Terahertz Rain Attenuation Model simulator, the authors have thoroughly investigated the rain-attenuation characteristics of terahertz signal in tropical climate condition for different hydrometeor properties including rain-rates and drop-size distribution. The effect of tropical thunderstorm has been uniquely incorporated by the authors in the present study along with atmospheric humidity and temperature based fluctuations. The reliability issues that are related with THz communication in tropical rain-fall have also been comprehensively analysed. Besides, a best-fit analysis has also been covered under different drop-size distribution statistics. It has been found that, in Indian Scenario (as a part of tropical climate), the peak attenuation level of THz spectrum under tropical rain-fall can be found in the range of (7THz-9THz). With increase of rain-rate from 2mm/hr to 200mm/hr, the peak attenuation level rises from ~100dB/km to ~1000dB/km. The basic model has been validated through experimental data where close proximity (with $\pm 10\%$ variation from the mean data) has been observed. The present study on terahertz signal attenuation profile in tropical rainy weather will help the communication engineers to open the new door for the ultra-high speed world of 6G terahertz communication.

INDEX TERMS Terahertz, Mie-theory, rain-attenuation, droplet-distribution, rain-rate, diffusion mass, growth-rate, reliability analysis.

I. INTRODUCTION

As per Edholm's law, the data-rate and bandwidth utilization double every 18 months, therefore the ever-increasing 'G' constraint (from 3G to 4G to 5G to...) has become a vibrant syndrome in today's communication scenario [1], [2], [3], [4],

The associate editor coordinating the review of this manuscript and approving it for publication was Barbara Masini¹.

[5]. The Terahertz (THz) spectrum occupies 0.1 THz to 10 THz bandwidth that can provide more flexibility in future wireless communication by initiating broader bandwidth, reduction in multipath effects and smaller equipment dimension, compared to millimeter wave regime. Besides, the non-invasive and non-ionizing properties of THz has expedited its necessity in defence applications. But, atmospheric turbulence can seriously affect the THz communication when beamed

from the source to the receiver-end. Cloud(s) is categorized under atmospheric aerosols. The Brownian deposition of ionized aerosols in cloud(s) leads to the coagulation of charges in cloud system [6], [7]. The effect of varying electrostatic forces inside cloud may lead to temporal variation in its charge-coagulation. This in turn enhances some adverse effects in the free space signal propagation in cloudy-atmosphere. Since water molecules can absorb THz signal drastically, the transmission of free space THz signals can be more susceptible to rain based attenuation. Therefore, due to the presence of water-laden cloud, that leads to precipitation, severe degradation in THz link availability occurs. The amount of THz signal attenuation due to rainfall depends primarily on the rainfall rate, which is often measured in millimeter per hour (mm/hour) unit. At THz regime, the rain induced signal attenuation can be considered to be a function of (a) signal frequency, (b) the intensity of rainfall with due adjustment of error function, (c) variations in rain drop size distribution including non-spherical shape of the rain drops and (d) temperature changes. The Rain Drop Size Distribution (RDS) has most important role in estimating the attenuation of THz signal when the same propagates through the rainy atmosphere [8], [9]. The water-vapour is the most significant lower atmospheric constituents which controls major weather phenomena. The amount of water vapour in Earth-atmosphere determines the possibility of rainfall. In the lower atmosphere, the concentration of water-vapour has profound spatial (altitude) and temporal dependence as well. The water vapour density ranges from a fraction of gram per cubic meter for very arid climates to approximately 30g/m^3 for hot and humid region [8], [9], [10]. Besides, the water vapour density in the lower atmosphere varies with atmospheric pressure and temperature. At an altitude of 1.5km from the surface of the Earth, the moisture density becomes half of the ground level. This density variation of water vapour leads to successive change in the refractive-index of the atmosphere through which the electromagnetic signal propagates.

The major part of Asia falls under the tropical climatic zone. In India, the effect of tropical climate leads to a temporal inhomogeneity in rainfall. Although the North-East and South-West monsoon govern the rainfall in India, the effect of North-East monsoon is limited within the Southern territory of this country. The mean diameter of tropical raindrops vary from 0.5mm to 5mm. In some cases, larger raindrops (diameters exceeding 5mm) have also been reported [11], [12]. In tropical climate zone the intensity of rainfall is very high and it is diverse in nature. THz signal fading can be profound under the tropical rain attenuation. The authors have highlighted the effects of rainfall on THz signal propagation in Fig.1. Based on weather condition and other atmospheric constraints, the computation of the rain based attenuation level of electromagnetic signal can be simulated by estimating the droplet population for a fixed radius interval and the extinction cross-section for an isolated raindrop at a particular radius. Besides the effect of rain-rate is also predominant in

enumerating the rain attenuation of electromagnetic signal. Several research works based on the ITU-R recommendation, have been carried out to find out the accurate rain-attenuation characteristics of electromagnetic signal [10], [11], [12], [13]. Besides, different theoretical models have also been reported in literature [14], [15], [16]. However to the best of authors' knowledge till date no report is available that covers rain attenuation characteristics of entire THz band within tropical climatic condition. Earlier, the authors have studied the fog attenuation characteristics of terahertz spectra and reported elsewhere [22]. This paper reports the details of Non-Linear Terahertz Rain Attenuation Model (NLTRAM) incorporating the effect of space and time dependent boundary conditions relevant for tropical climate zone to simulate the time-dependent variation of raindrop diameters. Moreover, for the occurrence of rainfall the combined effects of viscosity of atmosphere and the terminal velocity of rain drops are essential prerequisites. Unlike the fog-particles, the rain based aerosols experience sufficient downward force due to Earth's gravitational pull [17], [18]. The authors have also incorporated these natural force effects in this simulator. Besides, the effect of atmospheric pressure and temperature based variations of different constraints have been incorporated in this simulator. The effect of varying terminal velocities of rain-drops and scintillation have been initiated additionally. Moreover the reliability analysis on secure THz transmission in tropical climate region has also been carried out by the authors. In addition to the conventional Mie-theory analysis, the authors, have also incorporated the studies on THz signal attenuation due to the presence of thunderstorm in tropical climate scenario. Besides, based on experimental data on THz signal attenuation in the range of (0.1THz-1THz) for tropical climate scenario, a best-fit analysis has been additionally simulated by the authors under different Rain Drop Size Distribution Statistics (Weibull, Negative Exponential, Log-Normal, ITU-R). The results of this statistical analysis along with a tabular format on Root-Mean-Square Error (RMSE) calculations have been presented also by the authors uniquely in the present literature. The experimental validation of this model has been performed by comparing the experimentally observed data on rain based THz signal attenuation, obtained under other climatic situations with the simulation outcome for that different weather constraint.

As a part of major defence project in India, the authors, for the first time, have developed a non-linear, comprehensive and experimentally validated NLTRAM simulator to estimate the tropical rain based attenuation spectra of THz signal at various window frequencies. The outcome of this simulator would assist the defence people for establishing secure THz communication link in adverse weather scenario.

II. NUMERICAL ANALYSIS

The authors have incorporated time-dependent inhomogeneity in the indigenously developed NLTRAM simulator to simulate the rain based attenuation spectrum of THz signal

in tropical climate. The amount of atmospheric attenuation of electromagnetic signal primarily depends on the number distribution of aerosols under a specific climatic condition. As per the literature survey, this distribution statistics can be divided into two categories [17], [18], [19], [20] as

- i) Uniformly random-distribution.
- ii) Non-uniform distribution.

In case of uniform distribution statistics, the shape of rain-drops can be considered as spheres of a particular radius or fixed within a definite interval of radii, whereas the non-uniform distribution is based on random radius interval of droplets. In the NLTRAM simulator, the authors have considered composite distribution statistics for simulating the Rain Drop Size Distribution(RDSD) function, in which the effect of both of the above distribution characteristics are involved. The model analysis has been initiated by estimating the number distribution of rain-drops, $N(D_k)$, under the Law- Parsons distribution statistics, which can be expressed mathematically as

$$N(D_k) = N_m \exp(-\gamma D_k) \tag{1}$$

where, the slope-parameter γ varies inversely with rain-rate. It is expressed in mm^{-1} . The instantaneous drop-diameter D_k has the unit of mm and N_m is recognised as the intercept parameter of rain-drop size distribution, which is expressed in $\text{m}^{-3}\text{mm}^{-1}$. The intercept parameter depends primarily on the type of rainfall. Under continental thunderstorm, N_m can attain the level of $\sim 1500 \text{ m}^{-3}\text{mm}^{-1}$, whereas, the average value of this parameter is bounded within $\sim 8000 \text{ m}^{-3}\text{mm}^{-1}$. But the major disadvantage of this distribution statistics can be highlighted as adherence to temperate climate conditions. Upto 50mm/hr rain-rate variations, this statistics has a profound applicability to enumerate rain-based specific attenuation of electromagnetic signal in temperate climate zone. In tropical climate condition, Log-Normal Statistics of Rain-Drop Size Distribution, plays a very important role in predicting the rain-attenuation characteristics of free-space electromagnetic signals. The Log-Normal model can be expressed as,

$$N(D_k) = \frac{N_t}{\sigma D_k \sqrt{2\pi}} \exp \left[-0.5 \left\{ \frac{(\ln D_k - \mu)}{\sigma} \right\}^2 \right] \tag{2}$$

where, the number of rain-drops of all possible diameters can be introduced by N_t . Interms of μ and σ , the mean and standard deviation of $\ln D_k$ are expressed. All of these parameters depend on the rate of rainfall also. Incorporating the necessary weather dependent boundary conditions under tropical climate situation, the modified Method-of-Moment(MoM) technique has been applied by the authors for estimation of the parameters present in (2). Basically the third, fourth and sixth moments have been employed to simulate these parameters. Using modified MoM technique,

TABLE 1. List of major parameters incorporated in NLTRAM simulator.

Parameter	Physical Significance	Utility
f	Frequency	Terahertz regime
x	Size-parameter	Characterization of scattering
s	Radius	Droplet dimension
γ	Slope-parameter	RDSD estimation in tropical climate
N_m	Intercept-parameter	
D_k	k-th droplet diameter	
μ	Mean of $\ln(D_k)$ in Tropical Climate	
σ	SD of $\ln(D_k)$ in Tropical Climate	
g_{rr}	Rain-drop generation rate	Non-linearity in simulator
$t(s)$	Probability of rain-drop generation	
d_{sm}	Mean Nearest Neighbor Distance	
m_d	Diffusion mass	
\vec{V}_{fs}	Evaporation Flux Vector	
R_D	Non-resonant Dry Air Spectrum	Essential parameters to determine the complex refractivity of dispersive medium
R_C	Continuum Spectrum of Water Vapor	
R_W	Refractivity of Suspended water	
R_R	Contribution of falling aerosols	
T, T'	Air-blob and Atmospheric Temperature	
c_a, c_v	Thermal Conductivity Of dry air and water vapour	Reliability modeling
Z_v	Diffusivity of water-vapour	
ω_l	Liquid water entity	
$\xi(d, t, \varphi)$	THz Electric Flux-density of E-field	
L	Signal path Length	
p_{ri}	Exceedance probability	THz Rain based Attenuation Rate
A_{atmm}	Modified power-law application	

these parameters can be expressed as,

$$N_t = \exp [7.96M_3 - 9.2M_4 + 2M_6] \tag{3}$$

$$\mu = [-3.4M_3 + 4.6M_4 - 1.2M_6] \tag{4}$$

$$\sigma^2 = [0.67M_3 - 1.1M_4 + 0.4M_6] \tag{5}$$

In (3) to (5), M_3, M_4, M_6 are the natural logarithms of 3rd, 4th and 6th moments respectively. Since the rain-drops can be considered as falling aerosols with varying water entities, the absorption of electromagnetic signal(THz in this case), depend majorly on the liquid water content of these drops. To address the impact of this liquid water content in the indigenously developed NLTRAM simulator, the authors have incorporated time-dependent in-homogeneity by considering micro-crystals of aerosols. Besides, the authors have also incorporated the Weibull and Negative Exponential

distribution functions [19], [20], [21], [22], [23] with weather dependent parametric derivations to make a comparative study on the best-fit of rain-based attenuation spectra of THz signal in tropical climate. Since rain is also categorized as cloud droplets, the occurrence of which is one of the complex natural phenomenon, series of stochastic rain-drop growth and drop spacing events including and excluding thunderstorm, come to play. With reference to a fixed rain-drop treated as the source at a particular instant of time τ_k , the concept of the nearest neighbour principle [24], [25], [26], [27], [28] have been initiated in the simulator by considering the probability of finding the nearest neighbour of the source in between the locations s and $(s+ds)$ as $t(s)ds$. Since, the probability can be determined by the product of non-occurrence of rain-drop in between 0 to s and the probability of rain-drop occurrence in between s and $(s+ds)$, therefore, $t(s)$ can be expressed as

$$t(s) = 4\pi s^2 N(D_k, \tau_k) \left(1 - \int_0^s t(s) ds\right) \quad (6)$$

The generalized rain-drop generation rate g_{rr} can be expressed as

$$g_{rr} = \frac{t(s)}{4\pi s^2 N(D_k, \tau_k)} \quad (7)$$

Using (7) in (6), it can be found that

$$\frac{dg_{rr}}{g_{rr}} = -4\pi s^2 N(D_k, \tau_k) ds \quad (8)$$

By the help of (8), the rain-drop generation rate can be estimated as,

$$g_{rr} = g_0 \exp\left(-\frac{4}{3}\pi s^3 N(D_k, \tau_k)\right) \quad (9)$$

The term g_0 in (9) can be estimated from the maximum probability principle. From (9) it is clear that the localized concentration of rain-drops inversely vary with drop-intervals. The mean nearest neighbour distance can be determined using (9) as

$$d_{sm} = \left(\frac{81}{4\pi N(D_k, \tau_k)}\right)^{0.34} \int_0^\infty \left(\frac{4}{3}\pi s^3 N(D_k, \tau_k)\right)^{0.34} \times \exp\left(-\frac{4}{3}\pi s^3 N(D_k, \tau_k)\right) s^2 ds \quad (10)$$

Since the liquid water content ω_L (expressed in g/m^3) present in raindrops, can be approximated by the two sphere concept with one having the mean nearest neighbour distance, d_{sm} , (10) can be applied to predict the liquid water entity ω_L as,

$$\omega_L = \frac{0.8 * \exp(3 * \log r_c)}{d_{sm}^3} \quad (11)$$

where, r_c is the characteristic drop-radius. Since the atmospheric water droplets may comprise of static charges, the authors have generalized raindrop generation rate as expressed in (7) by mass-growth rate continuity. Incorporating the principle of Gaussian surface and evaporation flux

vector, this mass-growth rate can be expressed as [24], [25], [26], [27], and [28]

$$\frac{\partial m_d}{\partial t} = -4\pi \Delta_v [C_d + C'_d] (f_s - f_\infty) \quad (12)$$

In (12), m_d stands for the instantaneous mass of the water droplet, C_d and C'_d signify the drop-capacitances (without thunderstorm and with thunderstorm respectively), whereas the evaporation flux vector, at the surface of the water droplet can be expressed as $-\Delta_v \nabla_{f_s}$. In tropical weather scenario, the mean diameter of raindrops lie around 5mm and in some cases they are found also hydro-dynamically unstable. The authors, in this uniquely developed NLTRAM simulator, have incorporated the effect of composite distribution statistics by initiating the dependence of liquid water entity on the non-linear RSDS function as

$$\omega_L = \left(\frac{0.001\pi}{6}\right) * c_w * \int_0^\infty D_k^3 * N(D_k, \tau_k) dD_k \quad (13)$$

In (13), c_w signifies the density of fluid expressed in gm/cc . Given the weather dependent boundaries under tropical climate situation, thorough recursion based numerical process has been involved in the simulator to estimate the time dependent droplet distribution function. The intensity of rainfall, which is also known as rain-rate(\mathcal{R}), can be expressed as

$$\mathcal{R} = (0.0006\pi) * \int_0^\infty D_k^3 * N(D_k, \tau_k) * v(D_k, \tau_k) dD_k \quad (14)$$

In (14), $v(D_k, \tau_k)$ stands for the non-linear terminal velocity of the rain-drops [24], [25], [26], [27], [28].

A. RAIN-BASED ATTENUATION MODELING

The rain attenuation of electromagnetic signal can be simulated directly by using ITU-R prediction. As per the ITU-R prescribed model structure, the specific attenuation, A_t , of electromagnetic signal due to propagation through rain chamber can be expressed as [29], [30], [31], [32], [33], [34], and [35]

$$A_t \text{ (dB/km)} = \alpha \mathcal{R}^\beta \quad (15)$$

Equation(15) is basically a power-law in which α and β are the polarization coefficients, that can be expressed as

$$\alpha = 10^{\sum_{j=1}^4 a_j \exp\left\{-\left(\frac{\log_{10} f - b_j}{c_j}\right)^2\right\} + m_k \log_{10} f + c_a} \quad (16)$$

$$\beta = \sum_{j=1}^5 a_j \exp\left\{-\left(\frac{\log_{10} f - b_j}{c_j}\right)^2\right\} + m_l \log_{10} f + c_b \quad (17)$$

The coefficients used in (16) and (17) are provided in ITU-R datasheet. The effect of Rain-height and Slant-path play a very important role in estimating the rain-based attenuation level. However, the conventional ITU-R model has some basic limitations, in which the comparatively lower rain-rate and low frequency operability are the two basic issues.

The authors, in their indigenously developed NLTRAM simulator have incorporated the intensity distribution function [29], [30], [31], [32], [33], [34], [35] along with modified power-law to simulate the attenuation spectra of THz signal in rainy weather condition under tropical climate. For the vertically polarized Electric-field component of the incident electromagnetic wave within a rainy atmospheric medium, this function can be mathematically expressed as,

$$I_{vr} = \left| \sum_{i=1}^{\infty} \frac{2i+1}{i(i+1)} (a_1\pi_1 + b_1\tau_1) \right|^2 \quad (18)$$

whereas, the horizontally polarized counterpart can be expressed as,

$$I_{hl} = \left| \sum_{i=1}^{\infty} \frac{2i+1}{i(i+1)} (a_1\tau_1 + b_1\pi_1) \right|^2 \quad (19)$$

In (18) and (19) π_1 and τ_1 are the first-order angular scattering functions, whereas a_1 , b_1 stand for the standard Mie-Scattering parameters, described elsewhere [22]. Due to successive scattering processes from the falling hydrometeors, the resultant intensity I_{φ} of the fade-signal, as a function of scattering angle can be expressed as,

$$I_{\varphi} = \xi_0 \frac{\lambda^2}{(2\pi)^2} \{0.5 * (I_{vr} + I_{hl})\} \quad (20)$$

In Equation(20), ξ_0 stands for the amplitude of the incident Electric-field. If the angular scattering cross-section of the falling hydrometeors be treated as S_{φ} , then

$$S_{\varphi} = 2\pi * \int_0^{\pi} I_{\varphi} \sin\varphi d\varphi \quad (21)$$

Utilizing (20), the scattering-efficiency factor can be expressed as,

$$\eta_{sct} = \frac{1}{s^2} * \frac{S_{\varphi}}{\pi} \quad (22)$$

Equation(21) helps to determine the complete extinction of the electromagnetic signal in due course of its propagation through rain laden atmosphere. The attenuation coefficient A_{atm} of the electromagnetic signal can be finally established as

$$A_{atm} = C * \int_0^{\infty} \eta_{ext} * \pi r_k^2 * N(D_k) dD_k \quad (23)$$

In (23), the term η_{ext} stands for the extinction coefficient that can be determined from (22) with the help of standard Mie-Coefficients. The factor C in (23) is below 0.005. To make the analysis more realistic, the authors have incorporated the time-dependence by initiating the rain-rate exceedance probability [32], [33], [34], [35] $p_{\mathcal{R}t}$. Under tropical weather scenario, this exceedance probability can be used to predict the heavy rain occurrences that include thunderstorm also. For the propagation of THz signal through rain-laden atmosphere in tropical adverse weather scenario, $p_{\mathcal{R}t}$ can follow an

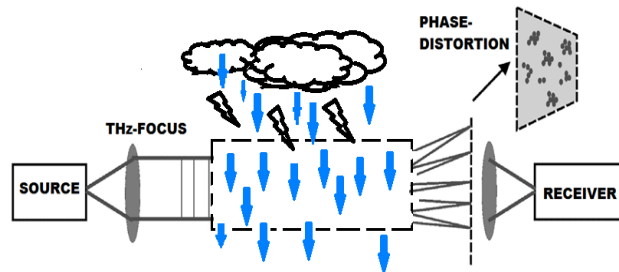


FIGURE 1. Effect of precipitation on the propagation of THz-wave.

inequality to estimate the effective path-length of the desired signal as,

$$0.477 * L^{0.633} * p_{\mathcal{R}t}^{0.073\alpha} * f^{0.123} - 10.579 * (1 - \exp(-0.024L)) \geq 0.4 \quad (24)$$

In (24), L stands for the actual path-length of the signal propagating through the rainy atmosphere and f denotes the signal frequency(THz). Considering the increase of the exceedance probability beyond 0.01% of time, the modified power-law [29], [30], [31], [32], [33], [34], [35] can be expressed as

$$\begin{aligned} A_{atm} &= A_{atm0.01} * \left\{ 0.07^{0.12+0.32*\log_{10}(0.1*f)} \right. \\ &\quad * 0.12^{1-\{0.12+0.32*\log_{10}(0.1*f)\}} \\ &\quad - [0.855 * \{0.12 + 0.32 * \log_{10}(0.1 * f)\} \\ &\quad + 0.546 (1 - \{0.12 + 0.32 * \log_{10}(0.1 * f)\}) + \\ &\quad \left. \left\{ 0.139 * \{0.12 + 0.32 * \log_{10}(0.1 * f)\} \right\} \right. \\ &\quad \left. \left\{ +0.043 (1 - \{0.12 + 0.32 * \log_{10}(0.1 * f)\}) \right\} \right\} \\ &\quad * \{ \tau * \log_{10} \tau \}. \end{aligned} \quad (25)$$

In (25) τ stands for the time-variable. The effects of vertical and horizontal polarizations have been incorporated by the authors also in the non-linear simulator to simulate the overall attenuation of the electromagnetic signal propagating through rain-laden atmosphere. If A_{atmH} and A_{atmV} represent the attenuation counterparts due to horizontal and vertical polarization respectively, then,

$$A_{atmV} = \frac{300 * A_{atmH}}{335 + A_{atmH}} \quad (26)$$

Besides the effect of scintillation [30], [31], [32], [33] due to the falling aerosols has been included by the authors also in the present simulator by initiating the predicted scintillation intensity and its weather-variant for tropical climatic boundaries [30], [31], [32], [33], [34], [35].

B. RELIABILITY MODELING

The authors have incorporated the reliability analysis in the indigenously developed NLTRAM simulator, by introducing the temperature, atmospheric pressure and humidity variations in the tropical climate condition. Since the heat-capacity

of water molecules with respect to that of the air-packet which is required to form the cloud, is negligibly small, a pseudo-adiabatic process is generated in due course of cloud formation and rainfall. The non-linear momentum equation of an air-packet at a particular temperature can be written as [35], [36], [37], [38], [39], [40], [41], [42], [43], [44], and [45],

$$\frac{d(mv)}{dt} = g(m' - m) - mg\omega_l \quad (27)$$

In (27), m stands for the mass of the air-packet, whereas m' signifies the atmospheric air mass displaced by the packet. ω_l and v denote the liquid water mixing ratio and the vertical velocity component of the air-packet respectively. Since the cloud based aerosols get activated to water drops which grow further by diffusion of water-vapour, the non-linear variation of the concentration of the water molecules in the air-packet can be expressed as,

$$\frac{\partial N}{\partial t} = -\mu\omega_l N + \frac{\partial N(\frac{activation}{deactivation})}{\partial t} + \frac{\partial N(\frac{condensation}{evaporation})}{\partial t} \quad (28)$$

In between the temperature range of $-40^{\circ}C$ to $+40^{\circ}C$, the diffusivity of atmospheric water [35], [36], [37], [38], [39], [40], [41], [42], [43], [44], [45] vapour can be expressed as

$$\mathbb{Z}_v = 0.211\left(\frac{T}{T_0}\right)^{1.94} * \left(\frac{p_0}{p}\right) \quad (29)$$

In (29), T_0 is $0^{\circ}C$, whereas p_0 is around 1013.25mb. The diffusivity is measured in cm^2sec^{-1} . If the thermal conductivity of dry air and water-vapour can be introduced by c_a and c_v respectively, then

$$c_a = (5.69 + 0.017 * T) * 10^{-5} \quad (30)$$

and

$$c_v = (3.78 + 0.020 * T) * 10^{-5} \quad (31)$$

The entrained blobs of an air-packet in the atmosphere can be assumed to evaporate a fraction of cloud-droplets of varying diameters until the relative-humidity appears the level of 100%. If the fraction of drops can be introduced by f_d , then

$$f_d = \frac{v_i}{\omega_l V} [\rho_{vsat}(T) - R_H \rho_{vsat}(T')] \quad (32)$$

In (32), v_i stands for the volume of i -th blob, V signifies the volume of the air-packet, $\rho_{vsat}(T)$, $\rho_{vsat}(T')$ signify the saturation concentrations of air-blob at temperature T and environmental temperature T' respectively. R_H stands for the relative-humidity. The authors have included the stochastic growth-decay process of rain-droplets in the simulator and the effect on the atmospheric propagation of THz signal to predict the most-reliable communication scenario. The complete flow-chart of the simulator has been shown in Figure 2. The authors, in Table 1, have summarized the parameters used in NLTRAM simulator. The complete flow-chart of NLTRAM simulator has been presented in Fig.2.

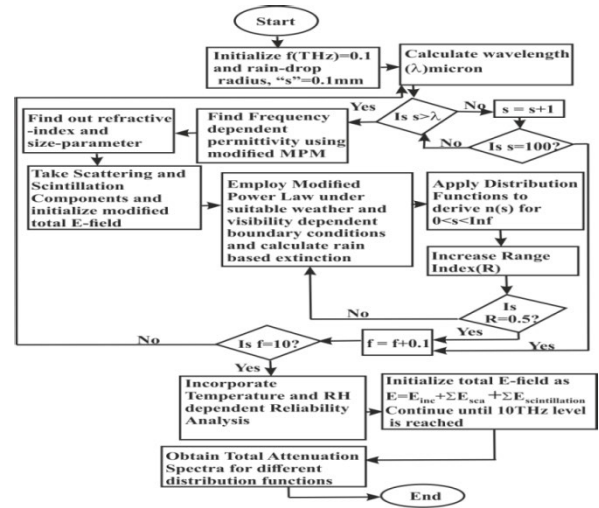


FIGURE 2. Flow-chart of NLTRAM Simulator incorporating reliability analysis.

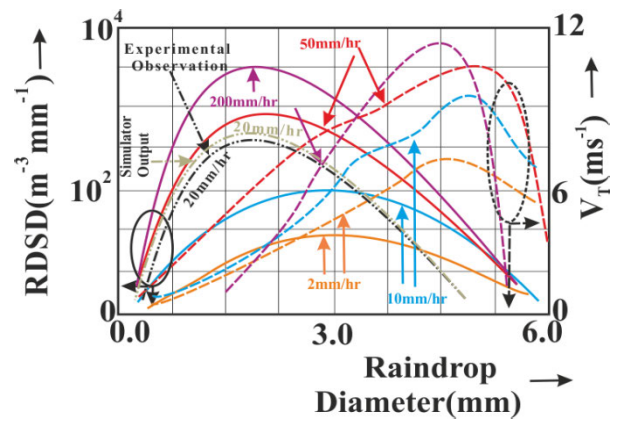


FIGURE 3. Rain Drop Size Distribution and variation of terminal velocity of droplets with raindrop diameter in tropical climate area(Comparison with Experimental Observation [25]has been included).

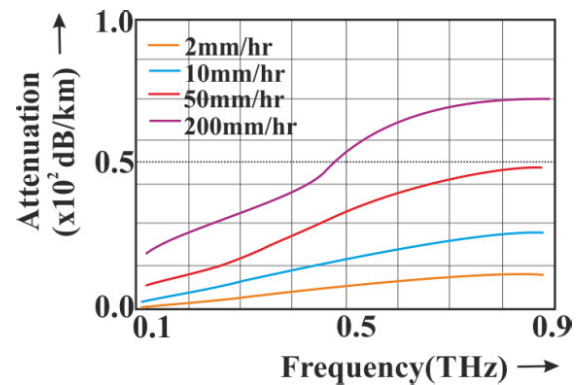


FIGURE 4. Rain based attenuation spectra of THz signal (below 1THz) for different rain-rates in tropical climate area.

III. RESULTS AND DISCUSSIONS

A. RAIN BASED ATTENUATION AND SCINTILLATION OF THZ SIGNAL IN TROPICAL CLIMATE

Prior to rain-based attenuation simulation of THz signal in tropical climate area, the authors performed the simulations

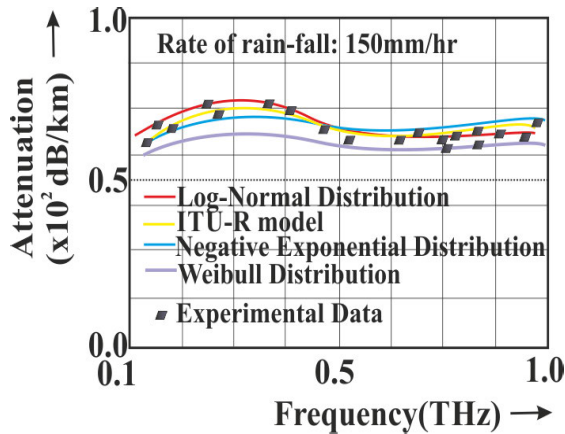


FIGURE 5. Variation of rain attenuation of THz signal for 0.1THz to 1.0THz for different RDSD compared with experimental observation [36].

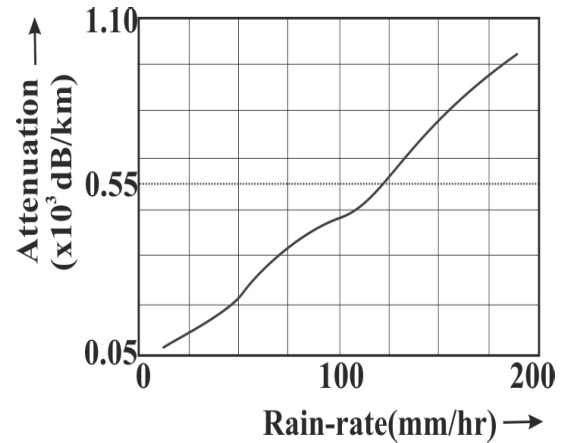


FIGURE 8. Variation of rain based attenuation of THz signal with different rain-rates in tropical climate area.

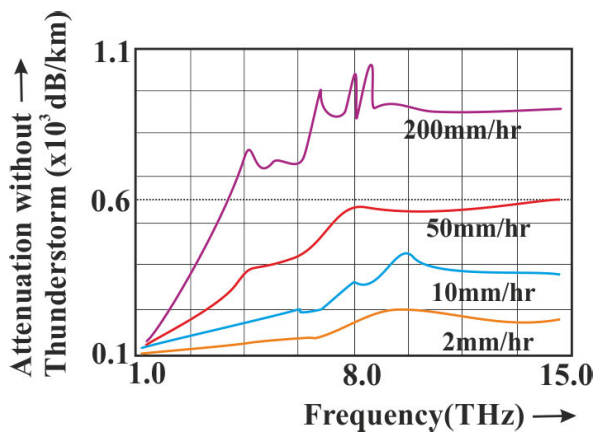


FIGURE 6. Rain based attenuation spectra (without thunderstorm effect) of THz signal (above 1THz) for different rain-rates in tropical climate area.

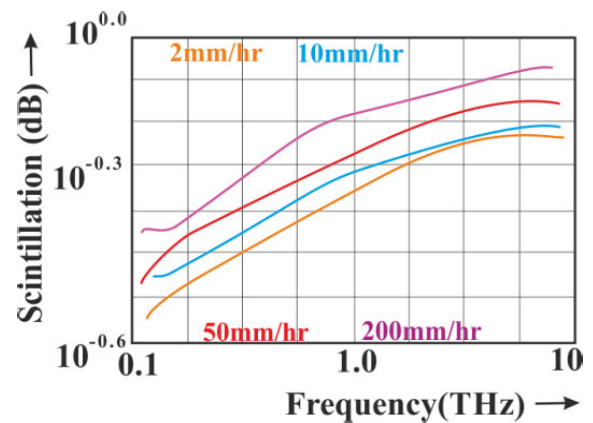


FIGURE 9. Variation of rain based scintillation of THz signal with different rain-rates in tropical climate area.

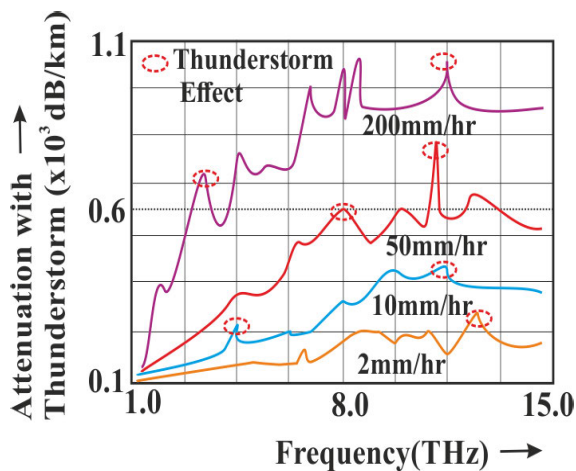


FIGURE 7. Rain based attenuation spectra (with thunderstorm effect) of THz signal (above 1THz) for different rain-rates in tropical climate area.

on the variations of RDSD along with the terminal velocity of water droplets with varying drop-diameters in tropical climate area under different rain-rates. The corresponding

variations have been presented in Fig. 3. As depicted in this diagram, it is clear that the mean diameter of water droplets around which the rain-drop population in tropical weather scenario can be treated maximum is approximately 3mm. As per the Log-Normal distribution statistics it is evident from the diagram that, the peak level of number distribution of water droplets around 3mm mean diameter can switch from $\sim 50\text{m}^{-3}\text{mm}^{-1}$ to $\sim 9000\text{m}^{-3}\text{mm}^{-1}$, when the rate of rain-fall increases from 2mm/hr to 200mm/hr in tropical climate condition. The authors have also compared the experimental data on rain-drop size distribution for Dehradun, India(Tropical climate) under 20mm/hr rate of rain-fall [25] with the simulator outcome for the same rain-rate, as shown in Fig.3. From this comparison it is clear that a close-proximity exists between the simulated and experimentally observed results, which establishes the validity of the simulator. The terminal velocity variations of the water droplets with rain-drop diameters, has been demonstrated also in Fig.3. It is clear from the figure that around 5mm average raindrop diameter, the droplets, under tropical climate condition, can achieve peak velocity. The drag-coefficient of atmosphere along with dynamic viscosity effects can be responsible in this respect

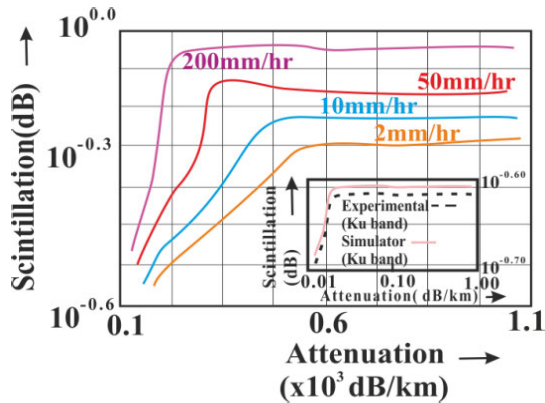


FIGURE 10. Variation of tropical rain based scintillation of THz signal as a function of THz attenuation for different rain-rates[Comparison with Experimental Observation at Ku-band [29] has been inscribed].

for this type of velocity spectrum of water droplets. The simulated rain-attenuation spectra for different rain-rates in the frequency range of 0.1THz to 0.9THz under tropical weather condition, have been shown in Fig.4, whereas Fig.6 and Fig.7 depict the same for the frequency range above 1THz. As evident from Fig.4, the nature of THz signal attenuation due to propagation through rainy atmosphere in tropical weather can be explained in terms of power-law. It is also clear from the diagram that within 0.5THz to 0.9THz, the attenuation spectra saturates for individual rain-rates. From Fig.4, the peak attenuation level of THz signal under tropical rain-fall has been found at the level of about 70dB/km with 200mm/hr average rain-rate, which decreases to ~ 10 dB/km for 2mm/hr rate value. Besides in Fig.5 the authors have shown the rain-based THz signal attenuation spectra for different RDS, as discussed in the previous section. Based on the experimental data obtained on the rain-attenuation rate of lower THz signal in tropical climate scenario [36], the authors have gone through a comprehensive error-analysis(RMSE) on different rain attenuation models. The results of this analysis have been presented in Table 2. It is evident from this diagram (Fig. 5) and Table 2 that the best fit is obtained for 0.25THz to 1.0THz frequency spectrum under Log-Normal distribution incorporating Mie-Scattering theory, whereas good-fit has been obtained under ITU-R prediction for 0.1THz, 0.5THz and 1.0THz frequencies in tropical climate scenario, under 150mm/hr rate of rain-fall. The outcome of this error-analysis has prompted the authors to perform further investigation on rain-based signal attenuation of higher THz regime(above 1THz) using Log-Normal RDS under tropical weather scenario. Compared to Fig.4, the nature of attenuation has been found somehow different in Fig.6, for the simulated frequency range above 1THz, where the effect of thunderstorm has not been considered. This can be well interpreted in terms of modified power-law effect, which has been already narrated in the mathematical modeling section. Based on time-dependent inhomogeneity and other weather dependent issues that explicitly vary with operating frequency of the signal, the outcome of the simulator exhibits typical fluctuations

in the attenuation spectra as shown in Fig. 6, compared to the flat nature shown in Fig. 4. It is clear from Fig. 6, that, the peak attenuation level jumps to ~ 1000 dB/km from ~ 100 dB/km, when the rain-rate increases from 2mm/hr to 200mm/hr. Unlike Fig. 4, the attenuation saturation bandwidth is also lower in Fig. 6 and a very high attenuation gradient has been found for 200mm/hr average rate of rainfall. Furthermore the authors have also incorporated the effect of thunderstorm in Fig. 7. Compared to Fig. 6, it is clear from this diagram that several spikes are associated in the attenuation spectra of THz signal passing through tropical thunderstorm with different rain rates. The generation of huge transient current within a very short duration of atmospheric discharge by thunderstorm cells can be responsible to explain these accidental impulses in the THz attenuation spectra. To the best of authors' knowledge this is the first report on the impact of tropical thunderstorm on THz attenuation spectrum. The authors have also shown the variations of rain-attenuation of THz signal with rain-rate under tropical climate scenario in Fig. 8. With increasing rate of average rainfall from 2mm/hr to 200mm/hr, it is clear from this diagram that the attenuation of THz signal also increases. The variation is following a ramp nature which is expected in lieu with Fig. 4, Fig. 6 and Fig. 7. The simulation results on rain-induced scintillations on THz signal propagation have been demonstrated in Fig. 9 and Fig. 10 for different rain-rates. It is clear from Fig. 9 that amount of rain-induced scintillation increases with frequency as well as rate of rain-fall, which satisfies the proportionality between scintillation and frequency. In Fig. 10, the authors have shown the effect of rain-induced scintillation fading on THz attenuation spectrum for different rate of rain-fall in tropical climate condition. It is clear from this diagram that, the rain-induced scintillation on THz signal can follow the similar nature of attenuation spectra, which can be estimated by using modified power-law. Strong scintillation can be found at tropical thunderstorm due to heavy ionization effects in atmosphere. To validate the model simulator, the authors have inscribed the comparison of simulated and experimentally observed rain-induced scintillation fade of Ku-band [29] signal obtained in South-African territory. It is evident from this figure that a very close proximity exists in between these two plots, that clearly establishes the viability of the simulator.

B. OUTCOME OF RELIABILITY ANALYSIS

To make a comprehensive reliability analysis of the THz communication system under tropical rain-fall, the authors initiated the model simulation with the temperature dependent variation of rain-drop size distribution. Since, the mean temperature of tropical climate lies around 65°F , the seasonal rainfall has widespread variations in its droplet dimensions. Fig.11 depicts the variation of rain-drop size distribution with environmental temperature (absolute), from which it is clear that the accumulation of rain-drops can be treated maximum approximately within (280K-300K) temperature domain. Munchak in 2012 [31] experimented on the raindrop

size distribution under the effect of atmospheric temperature fluctuation in tropical climate scenario using TRMM satellite data. From his valuable observation on long term rain statistics, it has been reported [31] that the presence of temperature in rainfall (tropical) can lead to enhancement of rain-drop diameters. As a part of tropical climate, in Indian scenario, according to the raindrop size-distribution statistics, the increase in droplet diameters leads to the degradation of rain-drop population, which has been clearly established by the current simulator output and shown in Fig. 11, which also establishes the validity of the present simulation study. In Fig. 12, the authors have established the variation of droplet size-distribution statistics with relative-humidity. It is clear from the figure that increase in atmospheric humidity leads to the enhancement of water droplets, which can reach the saturation level at a certain percentage of humidity-index. Since the rain-attenuation of electromagnetic signal (THz in the current analysis) majorly depends on the drop-size distribution statistics, both of Fig. 11 and Fig. 12 represent the reliability margins in terms of temperature and humidity fluctuations. From Fig. 11, it can be concluded that temperature above 280K can be treated as reliable operation region due to less growth probability of rain-droplets, whereas Fig. 12 highlights that approximate atmospheric humidity below 70% can be marked as safe-level for THz communication. In Fig. 13 and Fig. 14, the authors have shown the variations of THz attenuation with environmental temperature and atmospheric humidity. Similar to Fig. 11 and Fig. 12, in Fig. 13 and Fig. 14, the variations increase with rate of rain-fall. It is evident from Fig. 13 that the rain-attenuation may be considered as weak within fall rate of 50mm/hr in the temperature range of 300K to 320K. This can be interpreted in terms of moderate warm rain-fall in tropical weather scenario, where the population of rain-droplets may decrease with temperature enhancement [31]. On the other hand, the increase of rate rain-fall beyond 50mm/hr, can be considered as heavy or torrential. The increase in rate of rain-fall, in general, enhances the rain-based attenuation, where temperature can be treated as a catalyst beyond 50mm/hr. The large humidity in atmosphere can be associated with abundant droplets that may lead to successive decay of THz signal. The authors, in both of the figures Fig. 13 and Fig. 14, have shown the risk and safe zones for THz signal propagation in tropical climate on the basis of strong and weak attenuation effects respectively. In Fig. 15 and Fig. 16, the authors have shown the simulation results on the variations of diffusion mass growth-rate of liquid water crystals with atmospheric pressure and temperature in tropical climate scenario. The diffusion mass growth-rate of atmospheric aerosols in THz signal communication has a wide impact, which has been discussed earlier. As per Fig. 15, it is clear that with increasing atmospheric pressure or at the vicinity of Earth-surface, the growth-rate of water-crystals lowers down abruptly, which may ease the ground-based hopping of THz signal, whereas, Fig. 16 clarifies the temperature-bound on the growth-rate of liquid water crystals in tropical atmosphere. It is evident

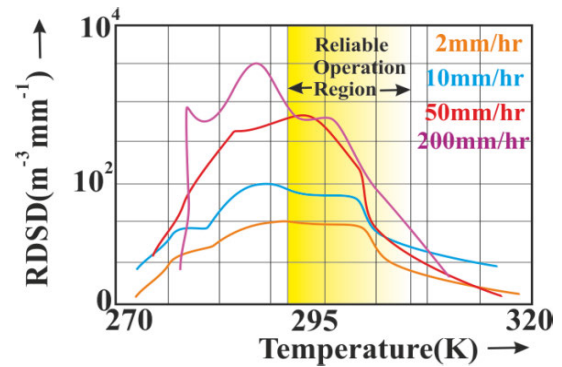


FIGURE 11. Variation of rain drop size distribution with environmental temperature for different rain-rates in tropical climate area.

from this figure that approximately within 260K to 290K, the growth-rate of crystals can be treated maximum, that can be quite harmful for THz communication. In connection with the diffusion mass growth-rate, the outcome of simulation on the variation of population-density of liquid water crystals, as depicted in Fig. 17, can be explained. The temperature belt in between 280K to 300K (under a particular level of humidity and atmospheric pressure in tropical weather condition), can be considered as the saturation regime for liquid water crystals, after which the natural vaporization can be incurred. Therefore, it is clear that, under tropical climate scenario, the winter-rainfall may lead to pronounced degradation of THz communication compared to autumn or pre-autumn rainfall. In Fig. 18, on the other hand, the authors have demonstrated the altitude based variations of liquid water crystal diameter and terminal velocity of droplets in tropical weather scenario. Since the falling aerosols break into particulates of lower dimensions due to the effect of gravity and atmospheric drag-force, the scattering and attenuation of THz signal may be feeble in the proximity of ground surface, while for THz LOS based communication set-up at a particular altitude from the earth-crust, severe disturbances may come due to the presence of condensed droplets of larger diameters. The variation of terminal velocity of droplets with altitude under tropical climate condition, as shown in the diagram, reveals that the velocity saturation of aerosols can be achieved at a certain height measured from the ground. Based on the dimension of water droplets and the saturation velocity margin, the 2km-4km altitude level, measured from the ground, in tropical climate scenario, can be treated as high risk zone in THz communication, due to profound interaction with the electromagnetic signal.

IV. EXPERIMENTAL VERIFICATION OF THE SIMULATOR

Initially the authors developed NLTRAM simulator by involving several parameters suitable for non-tropical rain-laden atmosphere. After that the model was compared with similar experimental observation reported by Federici et al [33]. Initially the authors developed NLTRAM simulator by involving several parameters suitable for non-tropical

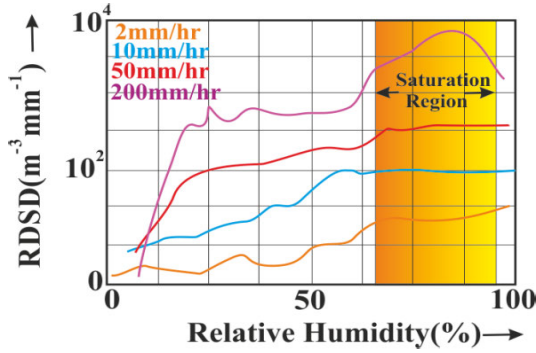


FIGURE 12. Variation of rain drop size distribution with relative humidity for different rain-rates in tropical climate area.

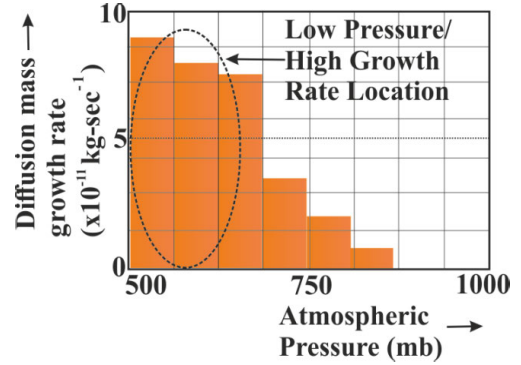


FIGURE 15. Variation of diffusion mass growth-rate of water droplets with atmospheric pressure in tropical climate area.

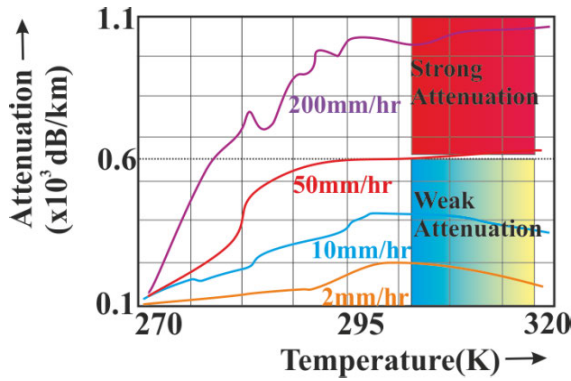


FIGURE 13. Variation of rain attenuation of THz signal with environmental temperature for different rain-rates in tropical climate area.

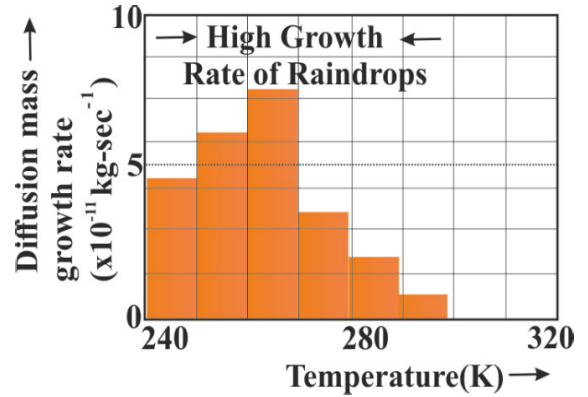


FIGURE 16. Variation of diffusion mass growth-rate of water droplets with environmental temperature in tropical climate area.

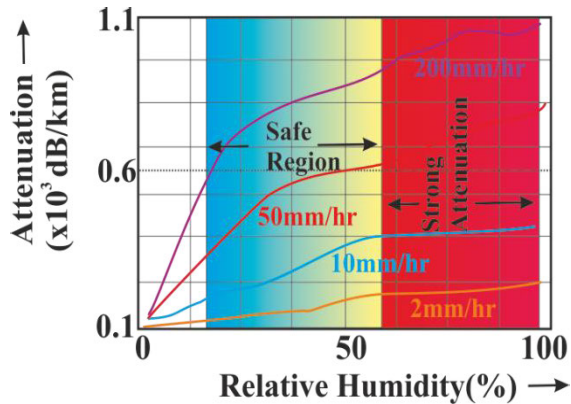


FIGURE 14. Variation of rain attenuation of THz signal with relative humidity for different rain-rates in tropical climate area.

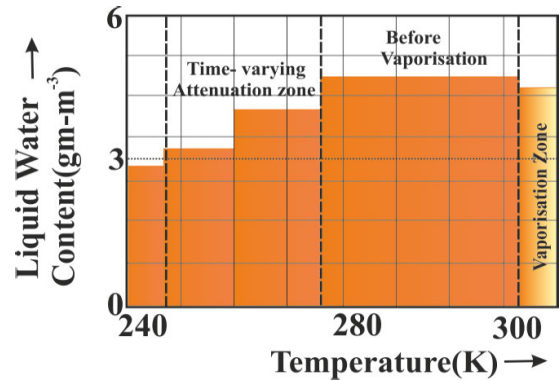


FIGURE 17. Variation of crystallographic water content of droplets with environmental temperature in tropical climate area.

rain-laden atmosphere. After that the model was compared with similar experimental observation reported by Federici et al [33]. It was found that the nature of attenuation spectrum of THz signal and the highest level of attenuation spectrum as obtained from the simulator are in close-proximity with the real-time experimental observation, that has been demonstrated in Fig.19. Furthermore, the authors have performed another comparison with the experimental observation on rain-attenuation spectrum of

THz signal in tropical climate situation. This experimental outcome has been reported by Tripathi et al [36] for lower THz frequency spectrum. The authors, incorporating weather dependent non-linear constraints for tropical climate scenario, simulated the rain-based THz attenuation model and the outcome has been presented in Fig. 20. It is evident from this diagram that there is also a close-agreement between the simulated and experimentally noticed THz attenuation levels in tropical climate. Thus the validation of the newly

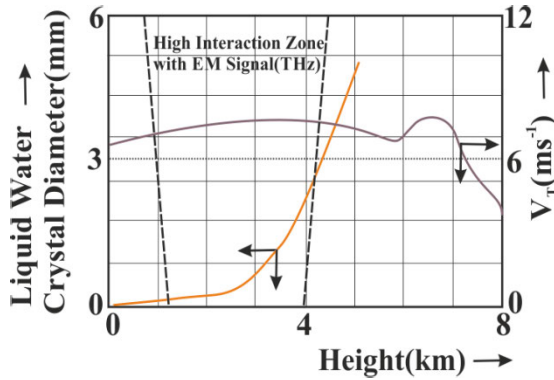


FIGURE 18. Variation of liquid water crystal diameter and terminal velocity of water droplets with altitude in tropical climate area.

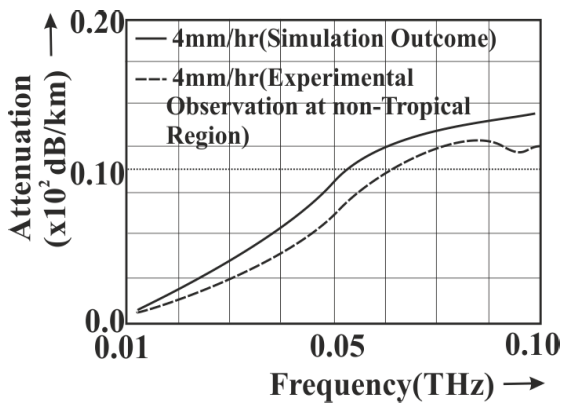


FIGURE 19. Rain based attenuation spectrum of THz signal in non-tropical climate zones, compared with experimental observation [33].

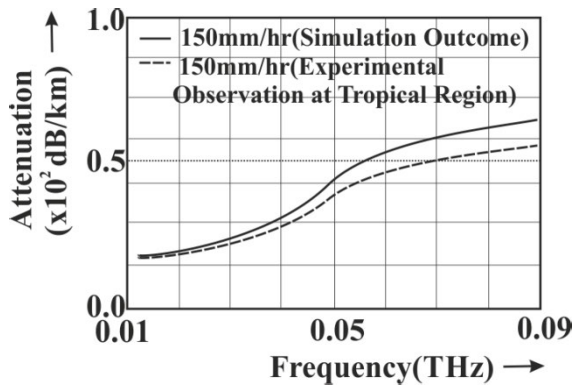


FIGURE 20. Rain based attenuation spectrum of THz signal in tropical climate zone, compared with experimental observation at lower frequency regime [36].

developed NLTRAM simulator has been achieved through a two-stage verification process: i) By comparing the experimental outcome in non-tropical weather scenario; ii) By comparing experimentally observed result with simulation outcome. In Fig.3 and Fig.10, as described by the authors' group in previous section, the comparison of the simulation outcome with experimental observations on RDS and rain-based scintillation have been clarified respectively.

TABLE 2. Comparison of RMS error (RMSE) in rain-attenuation spectra of THz signal (within 1.0THz) in tropical climate under different distribution functions.

Parameter	Frequency (THz)	Log-Normal	ITU-R	Weibull	Negative Exponential
RMS Error	0.10	0.32	0.56	4.25	0.24
	0.25	0.00	1.24	3.85	1.72
	0.50	0.81	0.78	2.42	0.15
	0.75	0.41	1.08	0.95	2.83
	1.00	0.47	0.53	1.52	2.54

In this way, the validation of the simulator has been established in the manuscript.

V. CONCLUSION

The authors, through an experimentally validated uniquely developed simulator, have established the effect of rain-based attenuation of THz signal in the tropical climate condition that includes Indian subcontinent. This has not been predicted by any other research-group till date. It has been clearly noticed from this work that, in Indian Scenario, the rain-based peak-attenuation level of THz signal follows a modified power-law structure that involves log-normal distribution of time-varying particle (liquid water droplet) concentration. The peak attenuation level of THz spectrum under tropical rain-fall can be found in the range of (7THz-9THz). The peak attenuation level rises from ~100dB/km to ~1000dB/km for increasing rain-rate from 2mm/hr to 200mm/hr. Newly developed NLTRAM simulator has been validated through experimental data where close proximity (with ± 10% variation from the mean data) has been observed. With increasing rain-fall rate, the attenuation increases. The outcome of rain-based scintillation also clarifies that the increase in rain-rate under Indian tropical climate scenario can expedite the signal-fading. Besides, the authors have performed the reliability analysis in THz signal propagation through tropical rain that can predict secure THz link establishment through falling aerosols. In future, comprehensive analysis on the THz attenuation simulation including Bit-Error Rate fluctuation and integrated simulation model with detailed atmospheric turbulence based applications can be incorporated under the influence of artificial intelligence and deep-learning. The outcome of this research will find its utility to develop secure link, for defence research in India.

ACKNOWLEDGMENT

The author Dr. Moumita Mukherjee wishes to acknowledge, Defence Research and Development Organization (DRDO),

Ministry of Defence, Government of India and Adamas University, for providing necessary infrastructure and facilities for conducting the research project. The authors wish to acknowledge Dr. U. C. Ray, Retd. Scientist-‘G’ and Advisor, SSPL-DRDO, Delhi, for his technical support and valuable guidance in the development of the model. They are willing to express their deepest thanks to the proof reader for the preparation of the revised manuscript.

REFERENCES

- [1] W. Feng, Y. Li, D. Jin, L. Su, and S. Chen, “Millimetre-wave backhaul for 5G networks: Challenges and solutions,” *Sensors*, vol. 16, no. 6, p. 892, Jun. 2016, doi: [10.3390/s16060892](https://doi.org/10.3390/s16060892).
- [2] E. Cianca, T. Rossi, A. Yahalom, Y. Pinhasi, J. Farserotu, and C. Sacchi, “EHF for satellite communications: The new broadband frontier,” *Proc. IEEE*, vol. 99, no. 11, pp. 1858–1881, Nov. 2011, doi: [10.1109/JPROC.2011.2158765](https://doi.org/10.1109/JPROC.2011.2158765).
- [3] T. Nagatsuma, “Exploring sub-terahertz waves for future wireless communications,” in *Proc. Joint 31st Int. Conf. Infr. Millim. Waves 14th Int. Conf. THz Electron.*, Shanghai, China, Sep. 2006, p. 4.
- [4] W. Gao, Y. Chen, C. Han, and Z. Chen, “Distance-adaptive absorption peak modulation (DA-APM) for terahertz covert communications,” *IEEE Trans. Wireless Commun.*, vol. 20, no. 3, pp. 2064–2077, Mar. 2021, doi: [10.1109/TWC.2020.3038902](https://doi.org/10.1109/TWC.2020.3038902).
- [5] L. Wang, G. W. Wornell, and L. Zheng, “Fundamental limits of communication with low probability of detection,” *IEEE Trans. Inf. Theory*, vol. 62, no. 6, pp. 3493–3503, Jun. 2016, doi: [10.1109/TIT.2016.2548471](https://doi.org/10.1109/TIT.2016.2548471).
- [6] B. A. Tinsley, “The global atmospheric electric circuit and its effects on cloud microphysics,” *Rep. Prog. Phys.*, vol. 71, no. 6, pp. 1–32, May 2008, doi: [10.1088/0034-4885/71/6/066801](https://doi.org/10.1088/0034-4885/71/6/066801).
- [7] S. Kumar, A. Hazra, and B. N. Goswami, “Role of interaction between dynamics, thermodynamics and cloud microphysics on summer monsoon precipitating clouds over the Myanmar coast and the Western Ghats,” *Climate Dyn.*, vol. 43, nos. 3–4, pp. 911–924, Aug. 2013, doi: [10.1007/s00382-013-1909-3](https://doi.org/10.1007/s00382-013-1909-3).
- [8] R. Piesiewicz, C. Jansen, D. Mittleman, T. Kleine-Ostmann, M. Koch, and T. Kürner, “Scattering analysis for the modeling of THz communication systems,” *IEEE Trans. Antennas Propag.*, vol. 55, no. 11, pp. 3002–3009, Nov. 2007, doi: [10.1109/TAP.2007.908559](https://doi.org/10.1109/TAP.2007.908559).
- [9] T. Wang, N. Zheng, J. Xin, and Z. Ma, “Integrating millimeter wave radar with a monocular vision sensor for on-road obstacle detection applications,” *Sensors*, vol. 11, no. 9, pp. 8992–9008, Sep. 2011, doi: [10.3390/s110908992](https://doi.org/10.3390/s110908992).
- [10] E. E. Altshuler and L. E. Telford, “Frequency dependence of slant path rain attenuations at 15 and 35 GHz,” *Radio Sci.*, vol. 15, no. 4, pp. 781–796, Jul./Aug. 1980, doi: [10.1029/RS015i004p00781](https://doi.org/10.1029/RS015i004p00781).
- [11] G. O. Ajayi and R. L. Olsen, “Modeling of a tropical raindrop size distribution for microwave and millimeter wave applications,” *Radio Sci.*, vol. 20, no. 2, pp. 193–202, Mar. 1985.
- [12] B. S. Jassal, A. K. Verma, and L. Singh, “Rain drop-size distribution and attenuation for Indian climate,” *Indian J. Radio Space Phys.*, vol. 23, pp. 193–196, Jun. 1994.
- [13] B. C. Gremont and M. Filip, “Spatio-temporal rain attenuation model for application to fade mitigation techniques,” *IEEE Trans. Antennas Propag.*, vol. 52, no. 5, pp. 1245–1256, May 2004, doi: [10.1109/TAP.2004.827501](https://doi.org/10.1109/TAP.2004.827501).
- [14] S. Das, A. Maitra, and A. K. Shukla, “Rain attenuation modeling in the 10–100 GHz frequency using drop size distributions for different climatic zones in tropical India,” *Prog. Electromagn. Res. B*, vol. 25, pp. 211–224, 2010, doi: [10.2528/PIERB10072707](https://doi.org/10.2528/PIERB10072707).
- [15] M. Marzuki, T. Kozu, T. Shimomai, W. L. Randeu, H. Hashiguchi, and Y. Shibagaki, “Diurnal variation of rain attenuation obtained from measurement of raindrop size distribution in equatorial Indonesia,” *IEEE Trans. Antennas Propag.*, vol. 57, no. 4, pp. 1191–1196, Apr. 2009, doi: [10.1109/TAP.2009.2015812](https://doi.org/10.1109/TAP.2009.2015812).
- [16] A. Tokay and D. A. Short, “Evidence from tropical raindrop spectra of the origin of rain from stratiform versus convective clouds,” *J. Appl. Meteorol. Climatol.*, vol. 35, no. 3, pp. 355–371, Mar. 1996.
- [17] I. Zawadzki and M. D. A. Antonio, “Equilibrium raindrop size distributions in tropical rain,” *J. Atmos. Sci.*, vol. 45, no. 22, pp. 3452–3459, Nov. 1988.
- [18] S. T. R. Pinho and R. F. S. Andrade, “An Abelian model for rainfall,” *Phys. A, Stat. Mech. Appl.*, vol. 255, nos. 3–4, pp. 483–495, Jul. 1998, doi: [10.1016/S0378-4371\(98\)00077-6](https://doi.org/10.1016/S0378-4371(98)00077-6).
- [19] A. Alonge and T. Afullo, “Rainfall drop-size estimators for Weibull probability distribution using method of moments technique,” *SAIEE Afr. Res. J.*, vol. 103, no. 2, pp. 83–93, Jun. 2012, doi: [10.23919/SAIEE.2012.8531962](https://doi.org/10.23919/SAIEE.2012.8531962).
- [20] D. S. Wilks, “Rainfall intensity, the Weibull distribution, and estimation of daily surface runoff,” *J. Appl. Meteorol.*, vol. 28, no. 1, pp. 52–58, Jan. 1989.
- [21] D. Chakraborty and M. Mukherjee, “Propagation of terahertz signal through tropical thunderstorm,” in *Proc. IEEE Int. Conf. Electron Devices Soc. Kolkata Chapter (EDKCON)*, Nov. 2022, pp. 190–194, doi: [10.1109/EDKCON56221.2022.10032876](https://doi.org/10.1109/EDKCON56221.2022.10032876).
- [22] D. Chakraborty and M. Mukherjee, “Self-consistent non-linear physics based predictive model for the computation of THz-signal attenuation in fog with varying visibility in tropical climatic zone,” *Microsyst. Technol.*, vol. 28, pp. 2611–2621, Mar. 2022, doi: [10.1007/s00542-022-05259-y](https://doi.org/10.1007/s00542-022-05259-y).
- [23] D. B. Akoma, J. S. Ojo, and O. Adetan, “Dynamical assessment of altitudinal trend of drop size distributions in a tropical region of Nigeria,” *J. Phys., Conf. Ser.*, vol. 2034, no. 1, Oct. 2021, Art. no. 012017, doi: [10.1088/1742-6596/2034/1/012017](https://doi.org/10.1088/1742-6596/2034/1/012017).
- [24] K. Parameswaran, K. O. Rose, and B. V. K. Murthy, “Relationship between backscattering and extinction coefficients of aerosols with application to turbid atmosphere,” *Appl. Opt.*, vol. 30, no. 21, pp. 3059–3071, Jul. 1991, doi: [10.1364/AO.30.003059](https://doi.org/10.1364/AO.30.003059).
- [25] A. K. Verma and K. K. Jha, “Rain drop size distribution model for Indian climate,” *Indian J. Radio Space Phys.*, vol. 25, pp. 15–21, Feb. 1996.
- [26] S. Vincent, E. Meillot, C. Caruyer, and J.-P. Caltagirone, “Modeling the interaction between a thermal flow and a liquid: Review and future Eulerian–Lagrangian approaches,” *Open J. Fluid Dyn.*, vol. 8, no. 3, pp. 264–285, 2018, doi: [10.4236/ojfd.2018.83017](https://doi.org/10.4236/ojfd.2018.83017).
- [27] R. M. Young and E. Pfender, “Nusselt number correlations for heat transfer to small spheres in thermal plasma flows,” *Plasma Chem. Plasma Process.*, vol. 7, no. 2, pp. 211–229, Jun. 1987.
- [28] J. A. Lewis and W. H. Gauvin, “Motion of particles entrained in a plasma jet,” *AICHE J.*, vol. 19, no. 5, pp. 982–990, Sep. 1973, doi: [10.1002/aic.690190515](https://doi.org/10.1002/aic.690190515).
- [29] A. G. Ashidi, J. S. Ojo, O. J. Ajayi, and T. M. Akinmoladun, “Evaluation of concurrent variation in rain specific attenuation and tropospheric amplitude scintillation over Akure, southwest Nigeria,” *Earth Syst. Environ.*, vol. 5, no. 3, pp. 547–559, Sep. 2021, doi: [10.1007/s41748-021-00225-6](https://doi.org/10.1007/s41748-021-00225-6).
- [30] A. Adhikari and A. Maitra, “Studies on the inter-relation of Ku-band scintillations and rain attenuation over an Earth-space path on the basis of their static and dynamic spectral analysis,” *J. Atmos. Solar-Terr. Phys.*, vol. 73, no. 4, pp. 516–527, Mar. 2011, doi: [10.1016/j.jastp.2010.11.010](https://doi.org/10.1016/j.jastp.2010.11.010).
- [31] S. J. Munchak, C. D. Kummerow, and G. Elsaesser, “Relationships between the raindrop size distribution and properties of the environment and clouds inferred from TRMM,” *J. Climate*, vol. 25, no. 8, pp. 2963–2978, Apr. 2012, doi: [10.1175/JCLI-D-11-00274.1](https://doi.org/10.1175/JCLI-D-11-00274.1).
- [32] D. Chakraborty and M. Mukherjee, “Terahertz window frequency signal attenuation and dispersion characteristics in tropical climate zone: An experimentally validated reliability analysis,” *IEEE Access*, vol. 10, pp. 54773–54783, 2022, doi: [10.1109/ACCESS.2022.3170480](https://doi.org/10.1109/ACCESS.2022.3170480).
- [33] J. Federici, L. Moeller, and K. Su, “Terahertz wireless communications,” in *Handbook of Terahertz Technology for Imaging, Sensing and Communications*. Amsterdam, The Netherlands: Elsevier, Mar. 2013, pp. 156–214, doi: [10.1533/9780857096494.1.156](https://doi.org/10.1533/9780857096494.1.156).
- [34] I. Shayea, T. A. Rahman, M. H. Azmi, and M. R. Islam, “Real measurement study for rain rate and rain attenuation conducted over 26 GHz microwave 5G link system in Malaysia,” *IEEE Access*, vol. 6, pp. 19044–19064, 2018, doi: [10.1109/ACCESS.2018.2810855](https://doi.org/10.1109/ACCESS.2018.2810855).
- [35] R. Harikumar, S. Sampath, and V. S. Kumar, “An empirical model for the variation of rain drop size distribution with rain rate at a few locations in southern India,” *Adv. Space Res.*, vol. 43, no. 5, pp. 837–844, Mar. 2009, doi: [10.1016/j.asr.2008.11.001](https://doi.org/10.1016/j.asr.2008.11.001).
- [36] S. Tripathi, N. V. Sabu, A. K. Gupta, and H. S. Dhillon, “Millimeter-wave and terahertz spectrum for 6G wireless,” in *6G Mobile Wireless Networks (Computer Communications and Networks)*. Springer, Mar. 2021.
- [37] H. Y. Lam, J. Din, and S. L. Jong, “Statistical and physical descriptions of raindrop size distributions in equatorial Malaysia from disdrometer observations,” *Adv. Meteorol.*, vol. 2015, pp. 1–14, Apr. 2015, doi: [10.1155/2015/253730](https://doi.org/10.1155/2015/253730).
- [38] S. Lavanya, N. V. P. Kirankumar, S. Aneesh, K. V. Subrahmanyam, and S. Sijikumar, “Seasonal variation of raindrop size distribution over a coastal station Thumba: A quantitative analysis,” *Atmos. Res.*, vol. 229, pp. 89–99, Nov. 2019, doi: [10.1016/j.atmosres.2019.06.004](https://doi.org/10.1016/j.atmosres.2019.06.004).

- [39] P. T. Dat, A. Bekkali, K. Kazaura, K. Wakamori, and M. Matsumoto, "A universal platform for ubiquitous wireless communications using radio over FSO system," *J. Lightw. Technol.*, vol. 28, no. 16, pp. 2258–2267, Aug. 2010, doi: [10.1109/JLT.2010.2049641](https://doi.org/10.1109/JLT.2010.2049641).
- [40] P. I. A. Kinnell, "Raindrop-impact-induced erosion processes and prediction: A review," *Hydrol. Processes*, vol. 19, no. 14, pp. 2815–2844, Sep. 2005, doi: [10.1002/hyp.5788](https://doi.org/10.1002/hyp.5788).
- [41] Y. Wu and L. Liu, "Statistical characteristics of raindrop size distribution in the Tibetan Plateau and southern China," *Adv. Atmos. Sci.*, vol. 34, no. 6, pp. 727–736, Apr. 2017, doi: [10.1007/s00376-016-5235-7](https://doi.org/10.1007/s00376-016-5235-7).
- [42] J. Federici and L. Moeller, "Review of terahertz and subterahertz wireless communications," *J. Appl. Phys.*, vol. 107, no. 11, Jun. 2010, Art. no. 111101, doi: [10.1063/1.3386413](https://doi.org/10.1063/1.3386413).
- [43] P. Squires, "The microstructure and colloidal stability of warm clouds. Part I—The relation between structure and stability," *Tellus*, vol. 10, no. 2, pp. 256–261, May 1958, doi: [10.1111/j.2153-3490.1958.tb02011.x](https://doi.org/10.1111/j.2153-3490.1958.tb02011.x).
- [44] H. Liebe, "Atmospheric EHF window transparencies near 35, 90, 140 and 220 GHz," *IEEE Trans. Antennas Propag.*, vol. AP-31, no. 1, pp. 127–135, Jan. 1983, doi: [10.1109/TAP.1983.1143013](https://doi.org/10.1109/TAP.1983.1143013).
- [45] Q. Jing, D. Liu, and J. Tong, "Study on the scattering effect of terahertz waves in near-surface atmosphere," *IEEE Access*, vol. 6, pp. 49007–49018, 2018, doi: [10.1109/ACCESS.2018.2864102](https://doi.org/10.1109/ACCESS.2018.2864102).



SAJITH D. NAIR received the M.Tech. degree in biomedical engineering, the CCE from IIT Kanpur, the M.Sc. degree, the AMIE degree, the PMP, and the C.Eng. degree. He is currently pursuing the Ph.D. degree with Adamas University. He has a professional membership with IEEE, IEEE-EMBS, and various other organizations. Moreover, he has several international certifications. He has successfully completed different government projects abroad.



MOUMITA MUKHERJEE (Member, IEEE) received the M.Sc. degree in physics with a specialization in electronics and communication, the M.Tech. degree in biomedical engineering, and the Ph.D. (Tech.) degree in radio physics and electronics from the University of Calcutta, India, in 2009. She did her doctoral and postdoctoral studies under DRDO, Ministry of Defence, Government of India. She was a Visiting Scientist and a Postdoctoral Researcher with INEX, Newcastle

University, U.K., and Technical University, Darmstadt, Germany. She was attached to the DRDO Centre under the Ministry of Defence, Government of India, as a Scientist (Reader grade), from 2009 to 2015. In continuation to that, she joined Adamas University, where she is currently a Professor with the Department of Physics and the Dean of Research and Development, after completing her terms as the Associate Dean and an Academic Coordinator, from 2016 to 2020, an Associate Professor, from 2017 to 2020, and an Assistant Professor, from 2015 to 2017, with Adamas University. With a total of 17 years of research and development and teaching experience, she is a Visiting/Adjunct Professor of JAP-BMI under Calcutta University and the West Bengal University of Health Sciences. She is also an alumnus of the R. K. S. M. Sister Nivedita Girls' School, Kolkata, the Presidency College, and Calcutta University. She is an empaneled examiner, a moderator, and a Ph.D. supervisor at public and private universities in West Bengal. She has guided more than 35 master's theses and 12 Ph.D. theses as a Supervisor/Jt. Supervisor. She has published more than 150 peer-reviewed research articles, to date, in reputed international refereed journals and reviewed proceedings with citation globally (citation: 900+ and H-index: 16). She is a principal investigator of five government (DRDO)- and start-up/industry-funded research projects worth 90 lakhs. Her research interests include THz electronics and communication, semiconductor devices, graphene electronics, photosensors, nanobiosensors, and medical electronics and instruments. She is a member of the IEEE ED Society and a Life Member of IEI, the Biomedical Society of India, and the Indian Science Congress.



DEBRAJ CHAKRABORTY was born in 1984. He received the M.Sc. degree in electronic science and the M.Tech. degree in radio physics and electronics from Calcutta University, in 2008 and 2010, respectively, and the Ph.D. (Tech.) degree in electronics and communication engineering from Adamas University, Kolkata, in 2022. He has more than ten years of experience in teaching. He is involved in the project work of DRDO, Government of India. He has several publications in SCI journals.